

# Approximate Solutions for Vibrations of Deploying Appendages

S. Kalaycioglu\* and A. K. Misra†

McGill University, Montreal, Quebec, H3A 2K6 Canada

The existing investigations of the dynamics of deploying appendages are numerical in nature. This paper presents approximate analytical solutions that may be used as "benchmarks" to check numerical solutions of more general equations of motion and for quick estimates in the early design phase. For beam-type appendages, approximate solutions are presented for uniform extension rate, exponential extension, and deployment when the square of the length varies linearly with time. For tethered systems, results for the common exponential deployment (or retrieval) are presented. The solutions provide new qualitative results that, during extension (or retraction), the amplitudes of transverse vibration of beam-type and tether-type appendages are proportional to  $L^{1/2}$  and  $L^{-1/4}$ , respectively, where  $L$  is the instantaneous length of the appendage. Thus, when the length is increasing during deployment, the vibratory amplitude of a beam increases whereas that of a tether decreases. The converse is true during retraction. The approximate solutions agree reasonably well with computer-intensive numerical solutions of more general equations.

## Introduction

THE vibrations of flexible appendages (beams, plates, or tethers) during their deployment from a spacecraft, as well as the attitude dynamics of spacecraft deploying flexible appendages, have received considerable attention in the past. For example, Barakat<sup>1</sup>, Tabarrok et al.,<sup>2</sup> and Jankovic<sup>3</sup> have examined vibrations of an axially moving rod representing a deploying spacecraft appendage. Cherchas and Gossain<sup>4</sup> have studied the dynamics of a flexible solar array during deployment from a spinning spacecraft. Attitude dynamics of a spacecraft deploying beam-type appendages was considered by Cherchas,<sup>5</sup> Lips and Modi,<sup>6,7</sup> and Tsuchiya,<sup>8</sup> and that of a spacecraft deploying plate-type appendages was analyzed by Ibrahim and Misra.<sup>9</sup> Deployment of an accordion-type appendage was studied by Djerassi and Kane.<sup>10</sup> Rotational and elastic motions of tether-connected systems during deployment and retrieval phases have been studied by Misra, Modi, et al.,<sup>11-13</sup> Banerjee and Kane,<sup>14</sup> and Arnold et al.<sup>15</sup> A rather general formulation, including various types of appendages, has been carried out by Modi and Ibrahim.<sup>16,17</sup> Recently, Banerjee and Kane<sup>18</sup> have presented a new method for simulating the vibrations of a beam being extruded from a retracted to a rotating base. As opposed to using shape functions (admissible functions) for discretization of the beam, as was the case for other investigators, they proposed to model the beam as a series of elastically connected rigid links.

The investigations mentioned above, except for one specific case in Tabarrok et al.<sup>2</sup> and a perturbation analysis in Jankovic,<sup>3</sup> have been numerical in nature. The reason for such a numerical study is that both inertial and stiffness characteristics of the appendages vary with time during their deployment. Thus, the partial differential equations governing the deployment dynamics, or the discretized ordinary differential equations, have time-varying coefficients and, in general, cannot

be solved analytically. However, there are several interesting and useful cases (i.e., several types of length variations) where approximate analytical expressions for vibratory displacements of deploying appendages can be obtained. This paper presents those solutions. The approximate solutions may be used as benchmarks to check numerical solutions of more general equations.

## Equations Governing Vibrations of Deploying Beam-Type Appendages

Consider a flexible appendage that can be modeled as a beam, undergoing deployment from a spacecraft (Fig. 1). The length of the appendage at any instant  $t$  is  $L$ . The appendage is assumed to be thin and inextensible, having a constant cross-sectional area  $A$  with moment of inertia  $I$  and mass per unit length  $m$ . The modulus of elasticity of the appendage material is  $E$ .

The flexural displacements of the beam at a distance  $y$  from the root are denoted by  $u$  and  $w$  along  $x$  and  $z$  directions, respectively. When the appendages are long and very flexible, there is a significant axial motion caused by the large trans-

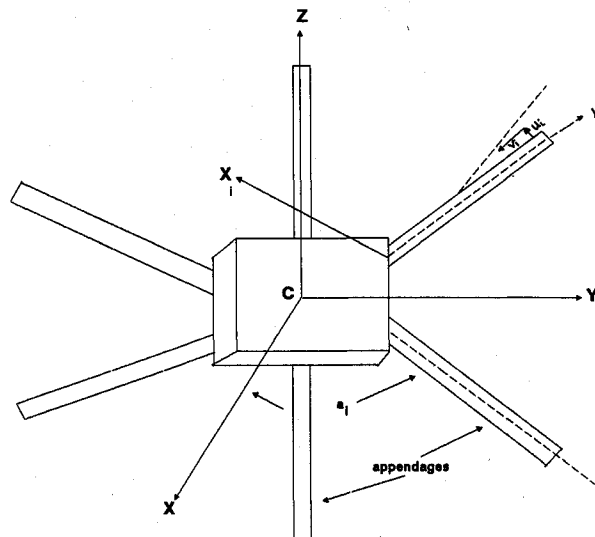


Fig. 1 Geometry of the system.

Presented as Paper 88-4250 at the AIAA/AAS Astrodynamics Conference, Minneapolis, MN, Aug. 15-17, 1988; received Oct. 25, 1988; revision received Nov. 17, 1989. Copyright © 1988 by S. Kalaycioglu and A. K. Misra. Published by the American Institute of Aeronautics and Astronautics, Inc., with permission.

\*Graduate Student, Department of Mechanical Engineering; currently, Systems Engineer, Thomson Systems, Canada. Member AIAA.

†Associate Professor, Department of Mechanical Engineering. Associate Fellow AIAA.

verse displacements. The axial translation  $v$  (toward the root) of an element at a distance  $y$  from the root is given by

$$v(y, t) = \frac{1}{2} \int_0^y \left[ \left( \frac{\partial u(y, t)}{\partial y} \right)^2 + \left( \frac{\partial w(y, t)}{\partial y} \right)^2 \right] dy \quad (1)$$

Clearly,  $v$  is a second-order quantity, and one might expect that it will have a negligible effect. However, this is true only if the central body of the spacecraft is nonspinning, as is the case here. In the case of spinning spacecraft, the axial translation has a significant effect and contributes nonnegligible quadratic terms to the kinetic energy expression.

The velocity of the element under consideration is given by

$$\dot{\mathbf{r}} = \begin{bmatrix} \dot{u} + \dot{L} \left( \frac{\partial u}{\partial y} \right) \\ \dot{L} - \dot{v} \\ \dot{w} + \dot{L} \left( \frac{\partial w}{\partial y} \right) \end{bmatrix} \quad (2)$$

which leads to the kinetic energy expression

$$T = \frac{1}{2} \int_0^L m \left[ \left( \dot{u} + \dot{L} \frac{\partial u}{\partial y} \right)^2 + (\dot{L} - \dot{v})^2 + \left( \dot{w} + \dot{L} \frac{\partial w}{\partial y} \right)^2 \right] dy \quad (3)$$

The terms  $\dot{L}(\partial u / \partial y)$  and  $\dot{L}(\partial w / \partial y)$  are convective components of the axial velocity  $\dot{L}$ . For the nonspinning case, the effect of nonlinear coupling between the axial translation and transverse displacement may be ignored, and  $v$  is dropped henceforth. The potential energy stored in the beam is given by

$$V = \frac{1}{2} \int_0^L EI \left[ \left( \frac{\partial^2 u}{\partial y^2} \right)^2 + \left( \frac{\partial^2 w}{\partial y^2} \right)^2 \right] dy \quad (4)$$

For convenience, the elastic displacements  $u$  and  $w$  are expanded in series forms as follows:

$$u(y, t) = \sum_{i=1}^n f_i(t) \phi_i[y, L(t)] \quad (5a)$$

$$w(y, t) = \sum_{i=1}^n g_i(t) \phi_i[y, L(t)] \quad (5b)$$

where  $\phi_i$ ,  $i = 1, 2, \dots, n$  form a set of shape functions satisfying at least the geometric boundary conditions, and  $n$  is the number of terms in the series expansions. In the present analysis, the shape functions are chosen as

$$\begin{aligned} \phi_i(y, L) &= L^{-1/2} \{ [\cosh \lambda_i(y/L) - \cos \lambda_i(y/L)] \\ &\quad - \sigma_i [\sinh \lambda_i(y/L) - \sin \lambda_i(y/L)] \} = L^{-1/2} \hat{\phi}_i \end{aligned} \quad (6a)$$

where

$$\sigma_i = (\cosh \lambda_i + \cos \lambda_i) / (\sinh \lambda_i + \sin \lambda_i) \quad (6b)$$

and  $\lambda_i$  are the roots of the equation

$$1 + \cosh \lambda \cos \lambda = 0 \quad (6c)$$

If the length were constant,  $\hat{\phi}_i$  would be the  $i$ th orthonormal eigenfunction (mode) of the appendage treated as a cantilever. For a variable length appendage, of course, there are no normal modes in the classical sense, and  $\hat{\phi}_i$  should not be interpreted as a mode. It is just a shape function. Note that  $\hat{\phi}_i$  has a nonzero time derivative, as it depends on  $L(t)$ .

Equations (5) and (6) are substituted in Eqs. (3) and (4) and Lagrange's equations are used to obtain the equations govern-

ing the generalized coordinates  $f_i(t)$  and  $g_i(t)$  that describe the transverse vibrations. The details of the algebra are omitted here for brevity. They are similar to that in Refs. 1-7, 16, and 17. The vector  $\mathbf{\tilde{f}}$  formed by the generalized coordinates  $f_i(t)$  satisfies the following matrix differential equation:

$$\ddot{\mathbf{\tilde{f}}} + 2(\dot{L}/L)\mathbf{\tilde{A}}\dot{\mathbf{\tilde{f}}} + [(\ddot{L}/L)\mathbf{\tilde{A}} - (\dot{L}/L)^2\mathbf{\tilde{B}} + \mathbf{\tilde{C}}]\mathbf{\tilde{f}} = \mathbf{\tilde{F}} \quad (7)$$

where the elements of the matrices  $\mathbf{\tilde{A}}$ ,  $\mathbf{\tilde{B}}$ , and  $\mathbf{\tilde{C}}$  and vector  $\mathbf{\tilde{F}}$  are as given below:

$$A_{ij} = \int_0^1 (1 - \xi) \hat{\phi}_i' \hat{\phi}_j' d\xi - (1/2) \delta_{ij} \quad (8a)$$

$$B_{ij} = A_{ij} + \int_0^1 (1 - \xi)^2 \hat{\phi}_i' \hat{\phi}_j' d\xi - (1/4) \delta_{ij} \quad (8b)$$

$$C_{ij} = \Lambda_{ij} = [EI/mL^4] \lambda_i^2 \lambda_j^2 \delta_{ij} \quad (8c)$$

$$F_i = 0 \quad (8d)$$

Here  $\xi$  is the nondimensional spatial coordinate ( $y/L$ ). Equation (7) is identical to that in Refs. 1-3. The integrals in Eqs. (8a) and (8b) can be evaluated by exploiting the properties of  $\hat{\phi}_i$ .

An equation similar to Eq. (7) is satisfied by the vector  $\tilde{\mathbf{g}}$  consisting of the generalized coordinates  $g_i(t)$ . Equation (7), of course, will be affected by the attitude dynamics. In the presence of an attitude control, however, the attitude motion is likely to be small for nonspinning satellites, and its effect on the vibrational equations is of the second order. (It can be neglected, at least in an approximate analysis such as this.) For spinning satellites,  $F_i$  in Eq. (8d) is nonzero, whereas the coefficients  $C_{ij}$  are slightly different.<sup>19,20</sup> The analysis can be similar, except that a particular solution must be obtained in addition to the homogeneous solution. This makes the analysis somewhat complicated and is not treated here, as the goal of this paper is to yield simple approximate solutions.

### Analytical Solutions for Beam-Type Appendages

Analytical solutions can be obtained for the vibratory displacements during deployment of a beam-type appendage if the length has certain specific variations with time. Here the satellite, of course, has been assumed to be nonspinning.

#### Uniform Extension

In this case, the deployment rate is constant and the length of the appendage at any time is given by

$$L = L_i + Vt \quad (9)$$

where  $L_i$  is the initial length and  $V$  is the deployment rate. Noting that  $\dot{L} = 0$ , Eq. (7) reduces to

$$\ddot{\mathbf{\tilde{f}}} + 2(\dot{L}/L)\mathbf{\tilde{A}}\dot{\mathbf{\tilde{f}}} + [-(\dot{L}/L)^2\mathbf{\tilde{B}} + \mathbf{\tilde{A}}]\mathbf{\tilde{f}} = \mathbf{\tilde{0}} \quad (10)$$

where  $\mathbf{\tilde{A}}$  is a square matrix whose elements are given by Eq. (8c). Note that  $\mathbf{\tilde{A}}$  is a diagonal matrix, but  $\mathbf{\tilde{A}}$  and  $\mathbf{\tilde{B}}$  have nonzero off-diagonal terms; thus, the generalized coordinates are coupled. This coupling, however, is small,  $\mathbf{\tilde{A}}$  being the dominant term, as  $\dot{L}/L$  is normally small. To obtain an approximate analytical solution, this coupling is ignored.

Defining a new time variable

$$\tau = L = L_i + Vt \quad (11)$$

the equation governing  $f_i$  can be rewritten as

$$\ddot{f}_i + \left( \frac{EI \lambda_i^4}{mV^2 \tau^4} - \frac{B_{ii}}{\tau^2} \right) f_i = 0 \quad (12)$$

where the dot now represents differentiation with respect to  $\tau$ .

Note that  $A_{ii} = 0$ . Equation (12) is in the form of

$$y'' + \frac{1}{x}(a + 2b x^p)y' + \frac{1}{x^2}[c + dx^{2q} + b(a + p - 1)x^p + b^2x^{2p}]y = 0 \quad (13)$$

and its solution is given by<sup>21</sup>

$$y = x^\alpha \exp(-\gamma x^p)[C_1 J_\nu(\beta x^q) + C_2 J_{-\nu}(\beta x^q)] \quad (14a)$$

where

$$\alpha = (1 - a)/2, \quad \beta = |d|^{1/2}/|q| \quad (14b)$$

$$\gamma = b/p, \quad \nu = [(1 - a)^2 - 4c]^{1/2}/(2|q|) \quad (14c)$$

Comparing Eqs. (12) and (13) and using Eq. (14), one notes that coefficients  $a$  and  $b$  are zero,  $q = -1$ , and the solution to Eq. (12) is given by

$$f_i(\tau) = \tau^\alpha [C_1 J_{\nu_i}(\beta_i/\tau) + C_2 J_{-\nu_i}(\beta_i/\tau)] \quad (15)$$

where  $\alpha = 1/2$ ,  $\nu_i = (1 + 4B_{ii})^{1/2}/2$ ,  $\beta_i = (EI\lambda_i^4/mV^2)^{1/2}$ , whereas  $C_1$  and  $C_2$  are constants that can be determined from initial conditions. The displacement  $u$  can now be determined by invoking Eq. (5a).

It may be of interest to note that  $\beta_i$  is quite large in practice and also that the argument  $\beta_i/\tau$  normally remains large throughout deployment. Thus, one can use the asymptotic expressions for Bessel functions with large arguments; i.e.,

$$J_\nu(x) = (2/\pi x)^{1/2} \cos(x - \pi/4 - \nu\pi/2)$$

Then, after noting that  $x = \beta_i/\tau$ ,  $\tau \equiv L$ ,  $f_i$  is given by

$$f_i = L^{1/2}(2L/\pi\beta_i)^{1/2} [C_1 \cos(\beta_i/L - \pi/4 - \nu_i\pi/2) + C_2 \cos(\beta_i/L - \pi/4 + \nu_i\pi/2)] \\ \equiv LD_i \cos(\beta_i/L + \Psi_i) \quad (16a)$$

Here,  $D_i$  and  $\Psi_i$  are two new constants of integration that can be determined from initial conditions. Then the elastic displacement is calculated as shown below.

$$u = \sum_{i=1}^n f_i \phi_i = \sum_{i=1}^n f_i L^{-1/2} \hat{\phi}_i \\ = L^{1/2} \sum_{i=1}^n D_i \hat{\phi}_i \cos(\beta_i/L + \Psi_i) \quad (16b)$$

Note that the oscillations are characterized by the argument  $\beta_i/L$ .

To check the accuracy of the analytical solution given by Eqs. (15) or (16), in conjunction with Eq. (5a), it was compared with the numerical solution of Eq. (7). The numerical solution was obtained for  $n = 3$ ; an IMSL routine DGEAR was used. Figure 2 compares the tip displacements of the beam-type appendage given by the numerical solution with the analytical solution (16b) with three terms in the series. The initial conditions have been chosen as follows:

$$f_i(0) = f_{i0} \text{ where } f_{10} = 2 \times 10^{-1}, f_{20} = 3 \times 10^{-2}$$

$$f_{30} = 7 \times 10^{-3}$$

$$\dot{f}_i(0) = (V/L_i) f_{i0}, \text{ where } V = 0.25 \text{ m/s and } L_i = 2 \text{ m}$$

The numerical values of the parameters are given in Table 1; the deployment/retrieval parameters are listed in Table 2. The initial velocities  $[\dot{f}_i(0)]$  have been chosen here such that in the analytical solution the constants of integration are easy to

Table 1 Appendage parameters used in the numerical calculations

Beam-type	
Diameter	0.0508 m
Thickness	$2.54 \times 10^{-4}$ m
Mass/unit length	0.599 kg/m
Bending stiffness	3798 Nm <sup>2</sup>
Tether-type	
Subsatellite mass	550 kg
Tether mass/unit length	$8.3 \times 10^{-3}$ kg/m

Table 2 Deployment/Retrieval Parameters

Uniform extension		Exponential extension	
Deployment time	592 s	Deployment time	592 s
Initial length	2 m	Initial length	2 m
Final length	150 m	Final length	150 m
Axial velocity	0.25 m/s	Coefficient $b$	$7.29 \times 10^{-3} \text{ s}^{-1}$
Square extension		Exponential retrieval (tether-type)	
Deployment time	592 s	Deployment time	5000 s
Initial length	2 m	Initial length	20 000 m
Final length	150 m	Final length	3475.5 m
Coefficient $c$	38 m <sup>2</sup> /s	Coefficient $c$	$3.5 \times 10^{-4} \text{ s}^{-1}$
		Orbital angular velocity	$1.16 \times 10^{-3} \text{ rad/s}$

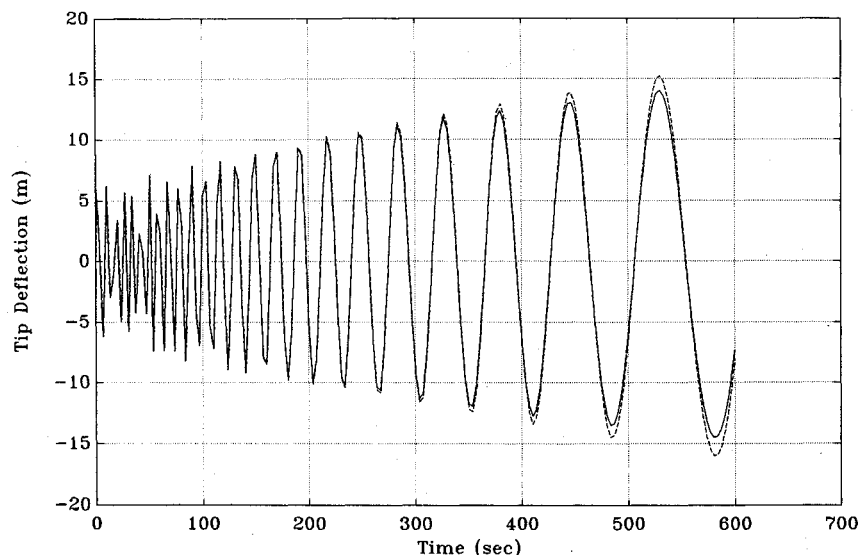


Fig. 2 Variation of tip deflection with time (uniform extension case, beam-type): ---- approximate analytical solution; — numerical solution.

find; however, this is not always necessary. It may be noted that the two curves in Fig. 2 are very close.

The discrepancy between the approximate analytical solution and the numerical solution increases as time increases. There are two possible reasons for this. When time ( $\tau$  or  $L$ ) increases, the argument  $\beta_i/\tau$  of the Bessel function in Eq. (15) becomes gradually smaller. Then the asymptotic cosine expression for the Bessel function with large argument is less accurate. The other reason may be that the error caused by neglecting  $A$  in Eq. (10) accumulates over time. Thus the damping is slightly off. A possible remedy may be to reinitialize after a certain time.

Since Eq. (7) is the same as in the works of Refs. 1-3, comparison of the analytical solution obtained here with the numerical solution of Eq. (7) is essentially a comparison of the present results with those of previous authors.

#### Exponential Extension

In exponential extension of appendages, the variation of length is given by

$$L = L_i \exp(bt) \quad (17)$$

As in the case of uniform extension, the coupling between the generalized coordinates is disregarded. Furthermore, one defines a new independent variable

$$\tau_e = \exp(-2bt) \equiv (L_i/L)^2 \quad (18)$$

The equation governing the generalized coordinate  $f_i$  can now be rewritten as

$$f_i'' + \frac{1}{\tau_e}(1 - A_{ii})f_i' + \left[ \beta_{ie}^2 - (\frac{1}{4})(\beta_{ii} - A_{ii}) \right] \tau_e^2 f_i = 0 \quad (19)$$

where prime denotes the differentiation with respect to  $\tau_e$ , and  $A_{ii}$  and  $B_{ii}$  are given by Eqs. (8a) and (8b), respectively, whereas  $\beta_{ie}$  is given by

$$\beta_{ie}^2 = E I \lambda_i^4 / (4b^2 m L_i^4) \quad (20)$$

Solution to Eq. (19) is given by

$$f_i = C_1 J_{\nu_i}(\beta_{ie} \tau_e) + C_2 J_{-\nu_i}(\beta_{ie} \tau_e) \quad (21a)$$

where

$$\nu_i = \frac{1}{4}(B_{ii} - A_{ii}) = \frac{1}{4}B_{ii}, \quad \text{since } A_{ii} = 0 \quad (21b)$$

Note that  $C_1$  and  $C_2$  can be obtained from the initial conditions.

Again, one can use the asymptotic form of Bessel functions, since  $\beta_{ie}$  is large in practice and  $f_i$  can be expressed as

$$\begin{aligned} f_i &= \left(2/\pi\beta_{ie}\tau_e\right)^{1/2} [C_1 \cos(\beta_{ie}\tau_e - \pi\nu_i/2 - \pi/4) \\ &\quad + C_2 \cos(\beta_{ie}\tau_e + \pi\nu_i/2 - \pi/4)] \\ &= (2/\pi\beta_{ie}L_i^2)^{1/2} L [C_1 \cos(\beta_{ie}L_i^2/L^2 - \pi\nu_i/2 - \pi/4) \\ &\quad + C_2 \cos(\beta_{ie}L_i^2/L^2 + \pi\nu_i/2 - \pi/4)] \\ &= LD_{ie} \cos(\beta_{ie}L_i^2/L^2 + \Psi_{ie}) \end{aligned} \quad (22a)$$

where  $D_{ie}$  and  $\Psi_{ie}$  are two new constants of integration. Here the oscillations are characterized by the argument  $\beta_{ie}L_i^2/L^2$  (varying as  $L^{-2}$  as opposed to  $L^{-1}$  in the uniform extension case), and the amplitude of  $f_i$  is proportional to  $L$  as in the previous case. Finally, elastic displacement  $u$ , of any point on the appendage, is calculated as

$$\begin{aligned} u &= \sum_{i=1}^n f_i \phi_i = \sum_{i=1}^n f_i L^{-1/2} \hat{\phi}_i \\ &= L^{1/2} \sum_{i=1}^n D_{ie} \cos(\beta_{ie}L_i^2/L^2 + \Psi_{ie}) \end{aligned} \quad (22b)$$

The analytical solution is compared with the numerical solution in Fig. 3. The difference between the two solutions is not significant, although the growth of discrepancy with time is observed again.

The initial conditions for the exponential deployment case are given below:  $f_i(0) = f_{i0}$  where  $f_{i0}$  are the same as in the uniform extension case, whereas  $\dot{f}_i(0) = b f_{i0}$ . The numerical values of deployment parameters are given in Table 2.

#### Extension with the Square of Length Varying Linearly with Time

Here, the length of the appendage varies with time according to the following equation:

$$L^2 = L_i^2 + ct \quad (23)$$

This is not a common deployment scheme, but it is shown in Ref. 19 that deployment, using Eq. (23), has a vibratory behavior superior to the previous two schemes.

It is easy to see now that  $\dot{L}/L = c/2L^2$ ,  $\ddot{L}/L = -c^2/4L^4$ , and Eq. (7) reduces to

$$\ddot{\mathbf{f}} + (c/L^2)\mathbf{A}\dot{\mathbf{f}} + (c^2/L^4)\mathbf{D}\mathbf{f} = \mathbf{0} \quad (24)$$

where  $\mathbf{D} = (L^4/c^2)\mathbf{A} - (\frac{1}{4})(\mathbf{A} + \mathbf{B}) = \text{const.}$

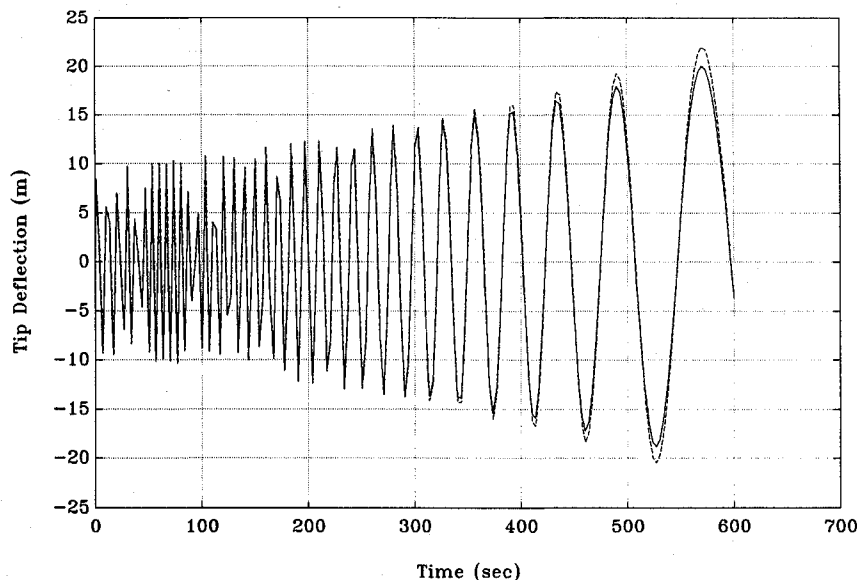


Fig. 3 Variation of tip deflection with time (exponential extension case, beam-type): ---- approximate analytical solution; — numerical solution.

It is convenient to define a new independent variable

$$\tau_s = L_i^2 + ct \equiv L^2, \quad \frac{d}{dt} \equiv c \frac{d}{d\tau_s} \quad (25)$$

Equation (24) then can be transformed to the form

$$\ddot{\mathbf{f}} + \frac{1}{\tau_s} \underline{A} \dot{\mathbf{f}} + \frac{1}{\tau_s^2} \underline{D} \mathbf{f} = \bar{0} \quad (26)$$

where prime stands for differentiation with respect to  $\tau_s$ .

It may be noted that Eq. (26) is of the Euler type and can be converted to a matrix equation with constant coefficients by defining another independent variable

$$s = \ln \tau_s \quad (27a)$$

so that

$$\frac{d^2 \mathbf{f}}{ds^2} + (\underline{A} - \underline{1}) \frac{d\mathbf{f}}{ds} + \underline{D} \mathbf{f} = \bar{0} \quad (27b)$$

where  $\underline{1}$  stands for the identity matrix.

In state space form, Eq. (27b) can be rewritten as

$$\frac{d}{ds} \begin{pmatrix} \mathbf{f} \\ \frac{d\mathbf{f}}{ds} \end{pmatrix} = \begin{pmatrix} \underline{0} & \underline{1} \\ -\underline{D} & \underline{A} - \underline{1} \end{pmatrix} \begin{pmatrix} \mathbf{f} \\ \frac{d\mathbf{f}}{ds} \end{pmatrix} \quad (28a)$$

or in abbreviated form

$$\frac{d}{ds} \tilde{\mathbf{q}} = \underline{H} \tilde{\mathbf{q}} \quad (28b)$$

where  $\underline{H}$  stands for the big square matrix on the right-hand side of Eq. (28a) and is constant, and  $\tilde{\mathbf{q}}$  is the state vector. Equation (28b) is a standard equation in linear algebra and the solution can be written formally as

$$\tilde{\mathbf{q}}(s) = \tilde{\mathbf{q}}(0) \exp(\underline{H}s) \quad (29)$$

Note that the exponential of the matrix  $\underline{H}s$  can be written in terms of the eigenvalues and the eigenvectors of  $\underline{H}$ .

Equation (29) is an exact solution of Eq. (24). It avoids numerical integration of differential equations; however, evaluation of exponential of a matrix requires the knowledge of its eigenvalues and eigenvectors. Although it is simpler to do the latter calculations, it still requires some numerical work. Since the spirit of this paper is to obtain short analytical expressions, an approximation similar to the previous two schemes is made; i.e., the small coupling between generalized coordinates is neglected. Then, from Eq. (27b) one obtains

$$\frac{d^2 f_i}{ds^2} - \frac{df_i}{ds} + D_{ii} f_i = 0 \quad (30)$$

where  $D_{ii} = (EI/mc^2)\lambda_i^4 - \frac{1}{4}B_{ii}$ . Use has been made of the fact that  $A_{ii} = 0$ . Solution of Eq. (30a), having constant coefficients, is given by

$$\begin{aligned} f_i &= \exp(s/2) A_i \cos[(D_{ii} - \frac{1}{4})^{1/2} s + \Psi_{is}] \\ &= \tau_s^{1/2} A_i \cos[(D_{ii} - \frac{1}{4})^{1/2} \ln \tau_s + \Psi_{is}] \\ &= L A_i \cos[2(D_{ii} - \frac{1}{4})^{1/2} \ln L + \Psi_{is}] \end{aligned} \quad (31)$$

Then

$$\begin{aligned} u &= \sum_{i=1}^n f_i L^{-1/2} \hat{\phi}_i \\ &= L^{1/2} \sum_{i=1}^n \hat{\phi}_i A_i \cos[(4D_{ii} - 1)^{1/2} \ln L + \Psi_{is}] \end{aligned} \quad (32)$$

where  $A_i$  and  $\Psi_{is}$  are determined from initial conditions. One may again note that the amplitude of the transverse oscillations during deployment grows as  $L^{1/2}$ . The oscillations in this scheme are characterized by a cosine term having an argument proportional to  $\ln L$ .

The solution as given by Eq. (32) (with three terms in the series) is compared in Fig. 4 with a numerical solution that uses three terms in the series expansion of Eq. (5a). The agreement seems to be quite good.

The initial conditions for this case have been chosen as follows:  $f_i(0)$  is the same as in the previous cases and  $\dot{f}_i(0) = \frac{1}{2}(c/L_i^2)f_{i0}$ . The values of the deployment parameters are given in Table 2.

### Analytical Solution for Tethered Systems

In this section, an analytical solution is obtained for transverse vibrations of tethers during deployment or retrieval of a tethered subsatellite. The equation of motion corresponding to this vibration can be written as<sup>13</sup>

$$\rho \frac{D^2 u}{Dt^2} - \frac{\partial}{\partial y} \left[ T(y) \frac{\partial u}{\partial y} \right] = 0 \quad (33)$$

where  $\rho$  is the mass-per-unit length of the tether. The tension in the tether is  $T(y)$ , and the operator  $D/Dt$  denotes the convective derivative  $(\partial/\partial t) + \dot{L}(\partial/\partial y)$ . The terms involving rotations have been ignored for the same reason as in the case of beams.

To discretize Eq. (33), one can express the transverse displacement  $u$  in series form similar to Eqs. (5):

$$u(y, t) = \sum_{i=1}^n f_i(t) \phi_i \left[ y, L(t) \right] \quad (34a)$$

where

$$\phi_i(y, L) = \sqrt{2} \sin(i\pi y/L) \quad (34b)$$

Note that again  $\phi_i$  has nonzero time derivative, since  $L$  varies with time. Substituting Eqs. (34) into Eq. (33), one obtains after some algebra

$$\ddot{\mathbf{f}} + 2(\dot{L}/L)\underline{A}\dot{\mathbf{f}} + [(\dot{L}/L)\underline{A} - (\dot{L}/L)^2\underline{B} + \underline{C}]\mathbf{f} = \bar{0} \quad (35)$$

which is of the same form as Eq. (7) except that the elements of the matrices  $\underline{A}$ ,  $\underline{B}$ ,  $\underline{C}$  are different here and are given by

$$A_{ij} = \int_0^1 (1 - \xi) \phi_i \phi_j' d\xi \quad (36a)$$

$$B_{ij} = 2A_{ij} - \int_0^1 (1 - \xi)^2 \phi_i \phi_j'' d\xi \quad (36b)$$

$$C_{ij} = (1/\rho L^2) \int_0^1 \phi_i (-T \phi_j'' - T' \phi_j') d\xi \quad (36c)$$

Here a prime denotes differentiation with respect to  $\xi (= y/L)$ . If tension  $T$  is assumed uniform,  $C_{ij} = (T/\rho L^2)ij \pi^2 \delta_{ij}$ .

An analytical solution is obtained now for the case of exponential retrieval, i.e.,

$$L = L_0 \exp(-ct) \quad c > 0 \quad (37)$$

The solution will be applicable to exponential deployment by simply changing the sign of  $c$ .

We now define a new variable as follows:

$$\tau = \exp(ct/2) \equiv (L_0/L)^{1/2} \quad (38)$$

and Eq. (35) can be rewritten as

$$\tau^2 \ddot{\mathbf{f}} + \tau(\underline{1} - 4\underline{A})\dot{\mathbf{f}} + [\tau^2 \underline{C} - 4(\underline{B} - \underline{A})]\mathbf{f} = \bar{0} \quad (39)$$

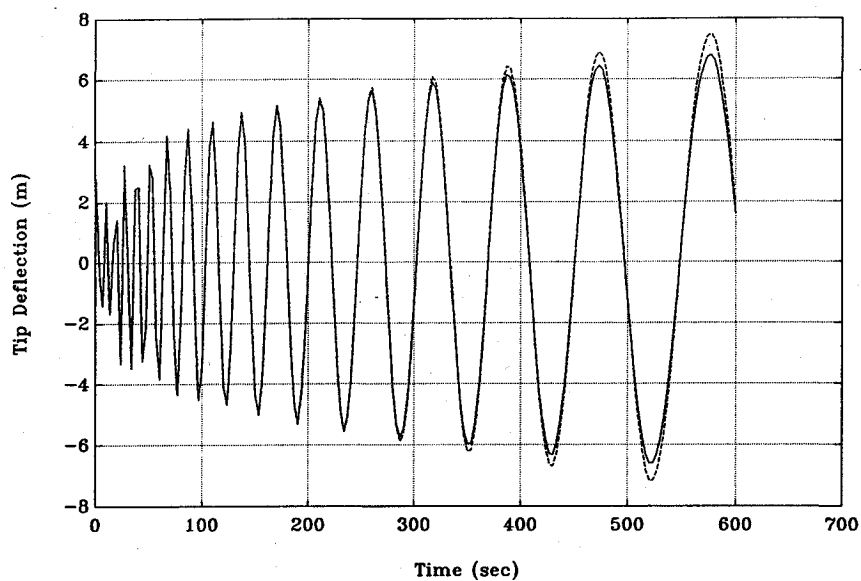


Fig. 4 Variation of tip deflection with time (extension with the square of length varying linearly with time, beam-type): ---- approximate analytical solution; — numerical solution.

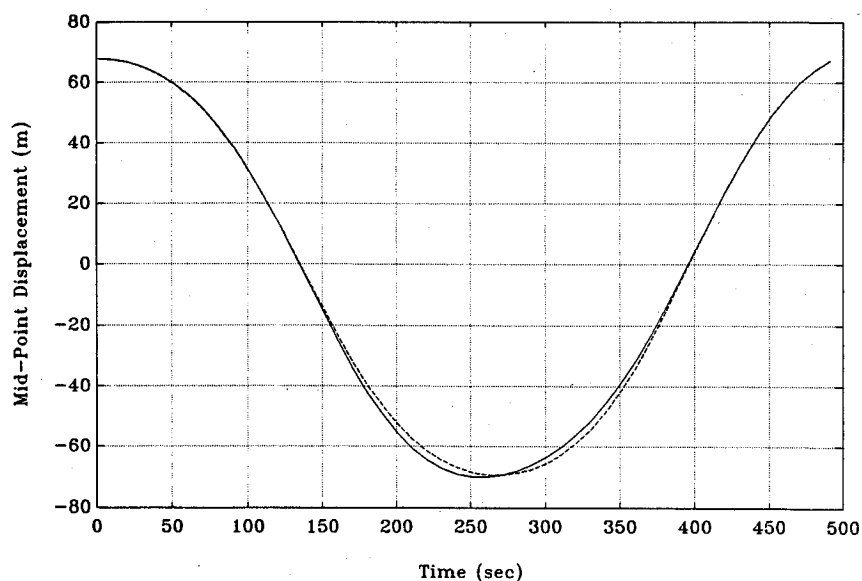
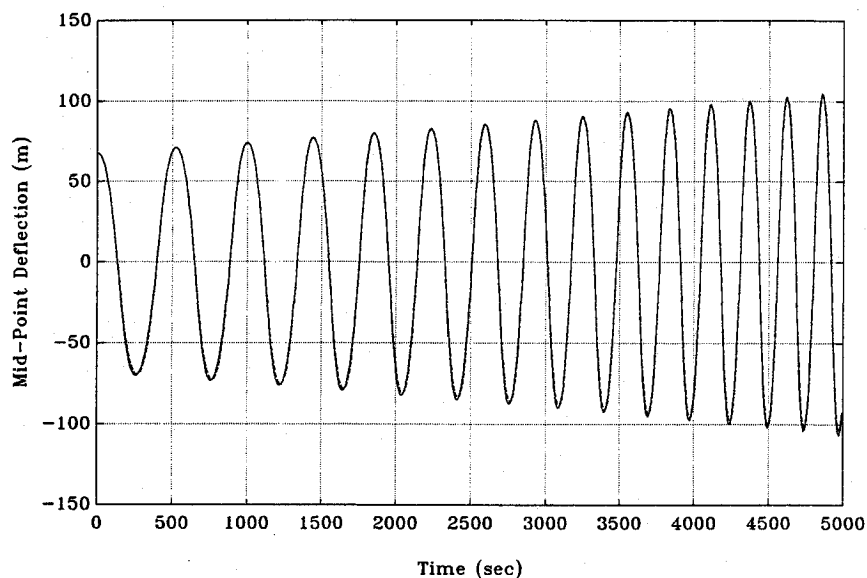


Fig. 5 Variation of midpoint deflection with time (exponential retrieval case, tether-type): ---- approximate analytical solution; — numerical solution.

where a prime now indicates differentiation with respect to  $\tau$ .

Note that the coefficients  $\hat{C}_{ij}$  are given by

$$\hat{C}_{ij} = (4/\rho L L_o c^2) \int_0^1 \phi_i(-T\phi_j'' - T'\phi_j') d\xi$$

Again, if one ignores coupling, tension is assumed uniform and equal to  $3m_s\Omega^2L$  and values of  $A_{ij}$  and  $B_{ij}$  are substituted, then Eq. (39) reduces to

$$\tau^2 f_i'' - \tau f_i' + [\lambda_i^2 \tau^2 - 4h_i] f_i = 0 \quad (40a)$$

where

$$\lambda_i = (2/c) i \pi \omega (3m_s/\rho L_o)^{1/2}, \quad h_i = i^2 \pi^2/3 \quad (40b)$$

The subsatellite mass is  $m_s$  and the orbital angular velocity is  $\omega$ . The solution to Eq. (40a) can be written in terms of Bessel functions as

$$f_i = \tau [C_1 J_{\nu_i}(\lambda_i \tau) + C_2 J_{-\nu_i}(\lambda_i \tau)] \quad (41)$$

where  $\nu_i = (1 + 4h_i)^{1/2}$  and  $C_1$  and  $C_2$  are arbitrary constants.

The arguments of the Bessel functions in Eq. (41) are quite large in magnitude in practice so that one can use asymptotic expressions for them. Thus,

$$\begin{aligned} f_i &= \tau (2/\pi \lambda_i \tau)^{1/2} [C_1 \cos(\lambda_i \tau - \pi/4 - \pi \nu_i/2) \\ &\quad + C_2 \cos(\lambda_i \tau - \pi/4 + \pi \nu_i/2)] \\ &= \tau^{1/2} D_i \cos(\lambda_i \tau + \Psi_i) \\ &= (L_o/L)^{1/2} D_i \cos[\lambda_i (L_o/L)^{1/2} + \Psi_i] \end{aligned} \quad (42)$$

where  $D_i$  and  $\Psi_i$  are to be obtained from initial conditions. The transverse displacement is then obtained using Eq. (34a) and is

$$u = (L_o/L)^{1/2} \sum_{i=1}^n \phi_i D_i \cos[\lambda_i (L_o/L)^{1/2} + \Psi_i] \quad (43)$$

Equation (43) states the interesting result that when the length changes, the amplitude of transverse oscillations varies as  $L^{-1/2}$ . This result is in agreement with a conclusion of Ref. 15 that was obtained from energy considerations. It is also interesting to note that  $\lambda_i (L_o/L)^{1/2}$  is equal to  $2\omega_i/c$ , where  $\omega_i$  is the "instantaneous"  $i$ th frequency of transverse oscillations. Thus, the transverse oscillations are not characterized by  $\sin(\omega_i t + \Psi_i)$  but by  $\sin(2\omega_i/c + \Psi_i)$ ; the dependence of the oscillatory term on time in this case appears indirectly through the variation of  $\omega_i$  with  $L$ .

Figure 5 compares the midpoint displacement of a tether-type appendage given by the numerical solution with the analytical solution (43), with three terms in the series. The initial conditions have been chosen as follows:  $f_i(0) = f_{i0}$  where  $f_{10} = 50$  m,  $f_{20} = 10$  m,  $f_{30} = 2$  m. Where  $d$  is the retrieval constant ( $c = 3.5 \times 10^{-4} \text{ s}^{-1}$ ),  $\dot{f}_i(0) = \frac{1}{4} c f_{i0}$ . The numerical values of parameters are given in Table 2. The initial length of the tether is 20 km, and the retraction takes place during 5000 s.

It may be noted that the two curves (numerical and approximate analytical) are very close. The discrepancy between the numerical and the approximate analytical solutions somewhat increases as time increases. Again, as in the case of approximate analytical solution of deploying beam-type appendage, the reason for this may be that the error due to neglecting the coupling in Eq. (39) accumulates over time.

### Conclusion

Approximate analytical solutions were obtained for transverse oscillations of deploying (or retracting) appendages of beam and tether types. The accuracy of the approximate solu-

tions as compared to the numerical solutions of more exact equations were found to be quite good.

An important observation was made that the amplitude of transverse oscillations during deployment or retraction varies as  $L^{1/2}$  for beam-type appendages, but as  $L^{-1/2}$  for tethered systems. Thus, during deployment, the vibrations of the beams increase while that of tethers decrease. The situation is reversed for retraction.

The analytical expressions obtained in this paper will serve as benchmarks to check numerical solutions of more general equations of motion, as well as for quick estimation of vibratory displacements in the early design phase.

### References

- Barakat, R., "Transverse Vibrations of a Moving Thin Rod," *Journal of the Acoustical Society of America*, Vol. 43, No. 3, 1968, pp. 533-539.
- Tabarrok, B., Leech, C. M., and Kim, Y. I., "On the Dynamics of an Axially Moving Beam," *Journal of the Franklin Institute*, Vol. 297, No. 3, 1974, pp. 201-220.
- Jankovic, M. S., "Lateral Vibrations of an Extending Rod," University of Toronto Institute of Aerospace Studies, Toronto, Canada, No. 202, June 1976.
- Cherchas, D. B., and Gossain, D. M., "Dynamics of Flexible Solar Array During Deployment from a Spacecraft," *CASI Transactions*, Vol. 7, 1974, pp. 10-18.
- Cherchas, D. B., "Dynamics of Spin-Stabilized Satellites During Extension of Long Flexible Booms," *Journal of Spacecraft and Rockets*, Vol. 8, No. 7, 1971, pp. 802-804.
- Lips, K. W., and Modi, V. J., "Transient Attitude Dynamics of Satellites with Deploying Flexible Appendages," *Acta Astronautica*, Vol. 5, No. 10, 1978, pp. 797-815.
- Lips, K. W., and Modi, V. J., "Three Dimensional Response Characteristics for Spacecraft with Deploying Flexible Appendages," *Journal of Guidance and Control*, Vol. 4, No. 6, 1981, pp. 650-656.
- Tsuchiya, K., "Dynamics of a Spacecraft During Extension of Flexible Appendages," *Journal of Guidance and Control*, Vol. 6, No. 2, 1983, pp. 100-113.
- Ibrahim, A. E., and Misra, A. K., "Attitude Dynamics of a Satellite During Deployment of Large Plate-Type Structures," *Journal of Guidance, Control, and Dynamics*, Vol. 5, No. 5, 1982, pp. 442-447.
- Djerassi, S., and Kane, T. R., "Equations of Motion Governing the Deployment of a Flexible Linkage from a Spacecraft," *Journal of the Astronautical Sciences*, Vol. 33, No. 4, 1985, pp. 417-428.
- Modi, V. J., and Misra, A. K., "On Deployment Dynamics of Tether Connected Two-Body Systems," *Acta Astronautica*, Vol. 6, No. 9, 1979, pp. 1183-1197.
- Misra, A. K., and Modi, V. J., "On Deployment and Retrieval of Shuttle Supported Tethered Satellites," *Journal of Guidance, Control, and Dynamics*, Vol. 5, No. 3, 1982, pp. 278-285.
- Misra, A. K., Xu, D. M., and Modi, V. J., "On Vibrations of Orbiting Tethers," *Acta Astronautica*, Vol. 13, No. 10, 1986, pp. 587-597.
- Banerjee, A. K., and Kane, T. R., "Tether Deployment Dynamics," *Journal of the Astronautical Sciences*, Vol. 30, No. 4, 1982, pp. 347-365.
- Arnold, D. A., Lorenzini, E. C., Kane, T. R., Modi, V. J., and Misra, A. K., "The Investigation of Tethered Satellite System Dynamics," Smithsonian Astrophysical Observatory, Cambridge, MA, Contract Rept., NAS8 36160, June 1987.
- Modi, V. J., and Ibrahim, A. E., "A General Formulation for Librational Dynamics of Spacecraft with Deploying Appendages," *Journal of Guidance, Control, and Dynamics*, Vol. 7, No. 5, 1984, pp. 563-569.
- Modi, V. J., and Ibrahim, A. E., "Dynamics of the Orbiter Based Construction of Structural Components for Space Platforms," *Acta Astronautica*, Vol. 12, No. 10, 1985, pp. 879-888.
- Banerjee, A. K., and Kane, T. R., "Extrusion of a Beam from a Rotating Base," AAS/AIAA Astrodynamics Conference, Kalispell, MN, American Astronautical Society Paper 87-477, Aug. 1987.
- Kalaycioglu, S., and Misra, A. K., "Optimal Deployment of Spacecraft Appendages," *Acta Astronautica*, Vol. 20, 1989, pp. 83-88.
- Kalaycioglu, S., "Dynamics of Satellites During Deployment and Retraction of Flexible Appendages," Ph.D. Dissertation, Dept. of Mechanical Engineering, McGill Univ., Montreal, Canada, 1988.
- Wylie, C. R., Jr., *Advanced Engineering Mathematics*, McGraw-Hill, New York, 1966, pp. 357-363.